Applications of the Transmission Line Matrix Method to Microwave Scanning Microscopy

Razvan Ciocan
Physics and Astronomy Department,
Clemson University, SC 29634-0978, USA
ciocan@clemson.edu

Nathan Ida
Electrical Engineering Department,
The University of Akron, OH 44325-3904, USA
ida@uakron.edu

Eugenia Ciocan
412 Old Central Rd # 4   SC 29631, USA
eugeniac1@yahoo.com

Huabei Jiang
Physics and Astronomy Department,
Clemson University, SC 29634-0978, USA
hjiang@clemson.edu

Abstract - **A three-dimensional transmission-line matrix (TLM) model was developed to simulate microwave-scanning microscopy. A TLM algorithm that allows the simulation of the scanning was developed. Numerical modeling was carried out for frequencies that are commonly used in microwave nondestructive testing (1GHz – 20GHz). Structures with local discontinuities in the electric permittivity are modeled numerically. The excitation parameters used in numerical modeling of scanning microwave microscopy were determined based on an initial frequency experimental response obtained from a plate with known permittivity. The numerical model developed in this paper is based on the symmetric condensed node. The description of the TLM algorithm is given in a Hilbert space using a three-index notation.**

I. INTRODUCTION

Microwave scanning microscopy is now one of the fastest growing areas among nondestructive methods. This method is applied in very different areas: aircraft industry, biological investigation, semiconductor industry and civil engineering. All these applications are based on the fact that microwave propagation is affected by a large number of material properties: composition, structure, moisture, delamination and presence of discontinuities. To make the microwave inspection a powerful tool in quantitative characterization of materials it is necessary to have a well-defined mathematical model of the testing problem. Because of the complexity of the problems, numerical methods were proven to give more appropriate models than analytical methods [1]. Microwave probes are robust enough to be placed in a hand-held configuration, which is the main advantage of microwave microscopy. Very high resolution can be achieved with probes that can work in-situ and on line. By comparison with other methods, currently used in nondestructive evaluation of materials, the advantages of the microwave microscopy are:

- Possibility to detect subsurface discontinuities.
- There are no problems related to material contamination caused by coupling.
- No physical contact is required between the probe and the material to be investigated; therefore the surface can be surveyed rapidly.
- No changes are caused in the material; the measurement is entirely nondestructive.
- In the microwave frequency region, variation of dielectric permittivity for dielectric materials is significantly larger than the contrast due to density.

The Transmission Line Matrix (TLM) as a time domain technique that can deal with complex geometries is one of the most suitable numerical methods to model microwave testing. Unlike some other numerical techniques, the TLM algorithm does not involve any convergence criteria, a property that makes it an inherently stable method. This stability is reflected in the flexibility of the TLM method when dealing with various types of input signals and boundaries. These advantages can be exploited for nondestructive investigation in several ways:

- A configuration can be numerically modeled in order to improve the experiment design and for a better understanding of the results obtained.

- The TLM method offers a versatile tool to reconstruct the initial signal based on the actual digitized signal, for homogeneous media.
- The TLM method can easily generate a time or frequency domain signal for known configurations. Based on this, a multi-layer structure can be fully characterized using an iterative process. The material parameters, of the multi-layer structure under investigation can be changed in the TLM model, so that the numerically generated signal fits the experimental signal.

The first published account of TLM method dates back to 1971 [2]. This and following publications demonstrated that TLM could be used in a wide range of applications. Almost 30 years after the first article was published, the method is considered to be "a modeling process rather than a numerical method for solving differential equations" [3]. The advantage of TLM is that it provides a direct simulation of the phenomenon and not of the equation governing it [4].

II. ALGORITHM DESCRIPTION

The TLM algorithm developed in this paper is based on Symmetrical Condensed Node (SCN) [5]. A description of the algorithm is given in a Hilbert space and it is based on a previous work [6]. This description was adapted to the three-index notation used consistently in numerical implementation. The use of this notation has two immediate advantages:

- A physical interpretation for the scattering matrix written in symmetrical notation is revealed [7].
- The equivalence between the classical notation and the three-index notation is obtained directly.

In Table 1 the first two rows and the last two columns were added in order to show the correspondence between the voltages used in the three-index notation (first row, last column) and the classical notation (second row, 13th column). The scattering matrix in symmetrical notation is obtained by changing the positions of rows and columns respectively in such a way that the initial scattering matrix is rewritten as a system of three four by four matrices [8]. The first two rows and last two columns in Table 1 show how the permutations between lines and columns, respectively, took place. The three-index notation shows that these permutations group together the voltages corresponding to each polarization. The factor of 1/2 that multiplies each element of the scattering matrix was omitted in Table 1 for space reasons. In Table 1, the constitutive matrices were colored in dark gray, light gray and white. The light gray matrix is the transpose of the dark gray matrix. These matrices can be rewritten in a symmetrical form by putting together the voltages (in the three-index notation) corresponding to each link line and polarization (Figure 1).

Table 1. Elements of scattering matrix in symmetrical notation.

V_{xny}	V_{xpy}	V_{xnz}	V_{xpz}	V_{ynz}	V_{ypz}	V_{ynx}	V_{ypx}	V_{znx}	V_{zpx}	V_{zny}	V_{zpy}		
3	11	6	10	5	7	1	12	2	9	4	8		
0	0	0	0	0	0	1	-1	0	0	1	1	3	V_{xny}
0	0	0	0	0	0	-1	1	0	0	1	1	11	V_{xpy}
0	0	0	0	1	1	0	0	1	-1	0	0	6	V_{xnz}
0	0	0	0	1	1	0	0	-1	1	0	0	10	V_{xpz}
0	0	1	1	0	0	0	0	0	0	1	-1	5	V_{ynz}
0	0	1	1	0	0	0	0	0	0	-1	1	7	V_{ypz}
1	-1	0	0	0	0	0	0	1	1	0	0	1	V_{ynx}
-1	1	0	0	0	0	0	0	1	1	0	0	12	V_{ypx}
0	0	1	-1	0	0	1	1	0	0	0	0	2	V_{znx}
0	0	-1	1	0	0	1	1	0	0	0	0	9	V_{zpx}
1	1	0	0	1	-1	0	0	0	0	0	0	4	V_{zny}
1	1	0	0	-1	1	0	0	0	0	0	0	8	V_{zpy}

Having this formulation for the scattering matrix, TLM can be represented by a numerable set of real quantities. A Hilbert space representation of the field state and evolution was introduced in [9]. Using this representation, the scattering matrix can be expressed by an operator as shown below. Considering the scattering matrix in symmetrical notation as given by Table 1, the scattering matrix operator, $\overline{S}$, is a real, symmetric and hermitian operator and it is written as
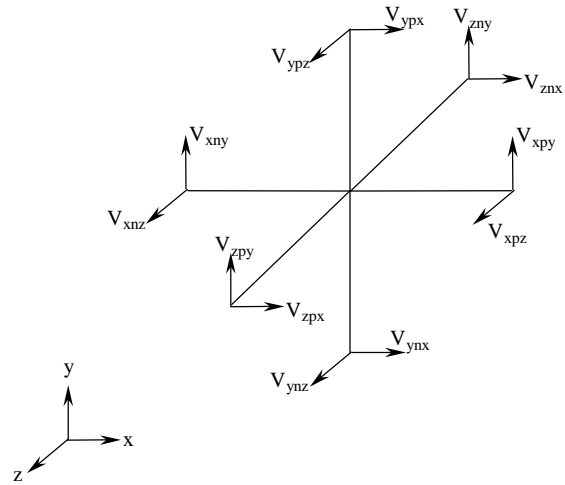
Figure 1. A schematic of SCN node.

$$\overline{S} = \begin{bmatrix} 0 & \overline{S}_0 & \overline{S}_0^T \\ \overline{S}_0^T & 0 & \overline{S}_0 \\ \overline{S}_0 & \overline{S}_0^T & 0 \end{bmatrix} \qquad (1)$$

with the matrix $\overline{S}_0$ given by

$$\overline{S}_0 = \frac{1}{2}\begin{bmatrix} 0 & 0 & 1 & -1 \\ 0 & 0 & -1 & 1 \\ 1 & 1 & 0 & 0 \\ 1 & 1 & 0 & 0 \end{bmatrix}. \qquad (2)$$

Consider the node with the discrete space coordinates (l, m, n). This corresponds to the space point of coordinates (x, y, z), with: $x=l\Delta x$, $y=m\Delta y$ and $z=n\Delta z$. At the discrete time coordinate k, corresponding to the time $t=k\Delta t$, all the incident and scattered wave amplitudes can be described using the 12-dimensional complex vectors of space C^{12}, $_k\overline{V^i_{lmn}}$ and $_k\overline{V^r_{lmn}}$ respectively. These vectors belong to a twelve dimensional complex vector space C^{12}, and are related, using the indices l, m n and k respectively, to the node with the discrete spatial coordinates (l, m, n) and to the temporal coordinate k. A Hilbert space, H_m, is introduced [8], having a system of orthonormal space domain vectors $|l,m,n\rangle$ assigned to each node positioned at (l, m, n). In a similar way a Hilbert space, H_t is introduced by associating the time coordinate k with the base vector $|k\rangle$. The Hilbert space where the TLM algorithm can be described is the Cartesian product of the previously introduced Hilbert spaces

$$H_w = C^{12} \otimes H_m \otimes H_t. \qquad (3)$$

In this space the incident and reflected amplitudes are written as

$$|V^i\rangle = \sum_{k,l,m,n=-\infty}^{\infty} {}_k\overline{V^i_{lmn}}|k;l,m,n\rangle, \qquad (4)$$

$$|V^r\rangle = \sum_{k,l,m,n=-\infty}^{\infty} {}_k\overline{V^r_{lmn}}|k;l,m,n\rangle. \qquad (5)$$

In the H_w space the following operators are defined:
- Time shift operator $\overline{T}$,

$$\overline{T}|k;l,m,n\rangle = |k+1;l,m,n\rangle. \qquad (6)$$

- X-shift operator ($\overline{X}$) and its Hermitian conjugate ($\overline{X}^*$),

$$\overline{X}|k;l,m,n\rangle = |k;l+1,m,n\rangle, \qquad (7)$$
$$\overline{X}^*|k;l,m,n\rangle = |k;l-1,m,n\rangle. \qquad (8)$$

- Y-shift operator ($\overline{Y}$) and its Hermitian conjugate ($\overline{Y}^*$),

$$\overline{Y}|k;l,m,n\rangle = |k;l,m+1,n\rangle, \qquad (9)$$

$$\overline{Y}^*|k;l,m,n\rangle = |k;l,m-1,n\rangle. \qquad (10)$$

- Z-shift operator ($\overline{Z}$) and its Hermitian conjugate ($\overline{Z}^*$),

$$\overline{Z}|k;l,m,n\rangle = |k;l,m,n+1\rangle, \qquad (11)$$

$$\overline{Z}^*|k;l,m,n\rangle = |k;l,m,n-1\rangle. \qquad (12)$$

- Connection operator ($\overline{\Gamma}$),

$$|V^i\rangle = \overline{\Gamma}|V^r\rangle. \qquad (13)$$

The connection operator shows that the reflected amplitudes are incident into the neighboring nodes and it is defined as

$$\overline{\Gamma} = \overline{X}\left(\overline{\Delta}_{xny,xpy} + \overline{\Delta}_{xnz,xpz}\right) + \overline{X}^*\left(\overline{\Delta}_{xpy,xny} + \overline{\Delta}_{xpz,xnz}\right) +$$
$$+ \overline{Y}\left(\overline{\Delta}_{ynz,ypz} + \overline{\Delta}_{ynx,ypx}\right) + \overline{Y}^*\left(\overline{\Delta}_{ypz,ynz} + \overline{\Delta}_{ypx,ynx}\right) + \qquad (14)$$
$$+ \overline{Z}\left(\overline{\Delta}_{znx,zpx} + \overline{\Delta}_{zny,zpy}\right) + \overline{Z}^*\left(\overline{\Delta}_{zpx,znx} + \overline{\Delta}_{zpy,zny}\right).$$

In Eq. (14) the matrices $\overline{\Delta}_{o,p}$ (o, p are each three- index notations defined in row 1 of Table 1) are 12 by 12 matrices and each element of these matrices $\left(\Delta_{i,j}\right)_{o,p}$ is defined as

$$\left(\Delta_{i,j}\right)_{o,p} = \delta_{i,o}\delta_{j,p}. \qquad (15)$$

The connection operator ($\overline{\Gamma}$) is a hermitian and unitary operator and therefore

$$\overline{\Gamma} = \overline{\Gamma}^{-1} = \overline{\Gamma}^*. \qquad (16)$$

The simultaneous scattering matrix at all TLM mesh nodes is described as

$$|V^r\rangle = \overline{T}\overline{S}|V^i\rangle. \qquad (17)$$

Eq. (17) shows that scattering by a TLM node causes a unit time delay Δt. The voltages defined in Figure 1 can be related to the tangential field components at the TLM node boundary by introducing the following vectors for each of the six faces of the TLM node:
- Reflected wave vectors,

$$\vec{V}^r_f = -\frac{1}{2}\left[\vec{n}_f \times \left(\vec{n}_f \times \vec{E}\right) + Z\vec{n}_f \times \vec{H}\right], \qquad f = \overline{1,6}. \qquad (18)$$

- Incident wave vectors,

$$\vec{V}_f^i = -\frac{1}{2}\left[-\vec{n}_f \times \left(\vec{n}_f \times \vec{E}\right) + Z\vec{n}_f \times \vec{H}\right], \qquad f = \overline{1,6}. \quad (19)$$

The correspondence between the node cube faces denoted by f in Eqs. (18) and (19), and the three-index notation is given in Table 2:

Table 2. The correspondence between the TLM node face notation (f index) and the three-index notation.

f index	1	2	3	4	5	6
Corresponding plane in three index notation	xn	xp	yn	yp	zn	zp

As an example, the plane xp (corresponding to $f=2$) from Table 2 is that located on the positive half of the x axis. This plane contains the voltages V_{xpy} and V_{xpz}. The normal to this plane is given by,

$$\vec{n}_2 = \begin{bmatrix} 1 & 0 & 0 \end{bmatrix}^T. \quad (20)$$

The field components in this plane are given by [6],

$$\vec{E} = \begin{bmatrix} {}_k[E_x]_{l+1/2,m,n} \\ {}_k[E_y]_{l+1/2,m,n} \\ {}_k[E_z]_{l+1/2,m,n} \end{bmatrix}, \quad (21)$$

$$\vec{H} = \begin{bmatrix} {}_k[H_x]_{l+1/2,m,n} \\ {}_k[H_y]_{l+1/2,m,n} \\ {}_k[H_z]_{l+1/2,m,n} \end{bmatrix}. \quad (22)$$

Substituting Eqs. (20) - (22) into Eqs. (18) and (19) the local reflected and incident wave vectors for a node located at (l,m,n) at moment k are given by [10]

$$_k\vec{V}_{2(l,m,n)}^r = \begin{bmatrix} 0 & V_{xpy}^r & V_{xpz}^r \end{bmatrix}^T, \quad (23)$$

$$_k\vec{V}_{2(l,m,n)}^i = \begin{bmatrix} 0 & V_{xpy}^i & V_{xpz}^i \end{bmatrix}^T. \quad (24)$$

The field quantities can be written in a more intuitive fashion in the three-index notation. For example, considering the notations in Figure 1, the components of the electric and magnetic fields are given by

$$E_x = -\frac{1}{2\Delta l}\left(V_{ynx}^i + V_{ypx}^i + V_{zpx}^i + V_{znx}^i\right), \quad (25)$$

$$E_y = -\frac{1}{2\Delta l}\left(V_{xny}^i + V_{xpy}^i + V_{zpy}^i + V_{zny}^i\right), \quad (26)$$

$$E_z = -\frac{1}{2\Delta l}\left(V_{xnz}^i + V_{xpz}^i + V_{ypz}^i + V_{ynz}^i\right), \quad (27)$$

$$H_x = \frac{V_{zny}^i - V_{ynz}^i + V_{ypz}^i - V_{zpy}^i}{2Z_o\Delta l}, \quad (28)$$

$$H_y = \frac{V_{xnz} + V_{zpx} - V_{xpz} - V_{znx}}{2Z_o\Delta l}, \quad (29)$$

$$H_z = \frac{V_{xpy} - V_{ypx} - V_{xyz} + V_{ynx}}{2Z_o\Delta l}. \quad (30)$$

The numerical implementation of a desired model is performed in three steps: pre-processing, computation and post-processing.

The pre-processing step includes determining the excitation signal parameters and generating the boundary coordinates of complex geometries. The excitation parameters in the TLM model are changed until a good fit is obtained between the experimental and numerical generated curves for a simple geometry. For instance, one experimental response was obtained from a bakelite plate. An appropriate numerical excitation that can give the same response as that obtained from this reflector was a Gaussian pulse with central frequency 1.6 GHz.

The processing step is made mainly of the TLM algorithm. The main steps of this algorithm are [11]: initialization, scattering and connection. An additional step called scanning was added to these components. This step involves changing the position of excitation according to the experimental scanning pattern whereby he TLM algorithm is repeated for each new position. The time response for each position is saved in an output file for further processing.

The programs developed for the post-processing part perform the following tasks:

- Reading the data input files generated by the processing program.
- Data visualization in two or three dimensions for each iteration considered.
- Signal processing of the numerically generated signal in time and frequency domain.

III. ALGORITHM IMPLEMENTATION

The scattering matrix implementation of the SCN used for this application is based on an algorithm that explores the symmetry of the scattering matrix [12]. The voltages in the port model for SCN can be assigned using a three-character name [13]. A representation for this node is given in Figure 1. In Figure 1 the first index denotes polarization (x, y or z), the second is related to position on the link line, positive or negative (p or n) and the last index is related to link line (x,

y or *z*). The voltages at all ports can be obtained considering all circular permutations of indices (*x,y,z*) denoted in general form as (*i,j,k*). These voltages are obtained according to the scattering matrix. To minimize the number of operations the reflected voltages at any port are obtained using the following scheme [14]

$$V_{inj}^{r} = V_{temp} - V_{dif} \, , \qquad (31)$$

$$V_{ipj}^{r} = V_{temp} \, . \qquad (32)$$

In Eqs. (31) and (32) the following notations were used

$$V_{temp} = \frac{1}{2}\left(V_{kni} + V_{kpi} + V_{dif}\right), \qquad (33)$$

$$V_{dif} = V_{ipj} - V_{inj} \, . \qquad (34)$$

The parameter used to obtain a microwave image is S_{11}. This parameter cannot be obtained directly from the TLM algorithm because an incident field cannot be separated. To solve this problem, two successive runs of the program are needed. The first run is performed with excitation without a reflecting object. This run will provide data for the reference port. A second run of the program will be performed considering boundary conditions for objects to be investigated. The S_{11} parameter is given by

$$S_{11} = \frac{F_i - F_0}{F_i + F_0} \, . \qquad (35)$$

In relation (35) F_0 and F_i are the frequency response obtained for the same position of excitation source without reflecting object and with reflector respectively.

IV. RESULTS

To validate the numerical model, the experimental set-up for microwave microscopy depicted schematically in Figure 2 was used. It consisted of a microwave resonator (open-ended coaxial line sensor) connected to a network analyzer. The probe was mounted horizontally over an *x-y* table. During the scanning process, the probe was held at a constant height over the sample (typically 10 μm) Stepper motors controlled via a serial interface by computer assured the positioning of the sample (the minimum step size was 1μm).
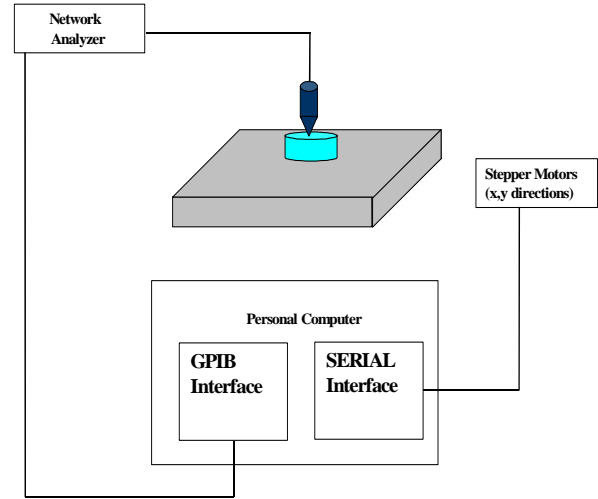
Figure 2. The experimental set-up used in microwave microscopy experiments.

Figure 3 shows the plot of the S_{11} parameter for three different materials: metal, bakelite (ε_r =5) and teflon (ε_r =2). The plot demonstrates the capability of the proposed TLM model to differentiate between materials with different electric permittivities. The frequency response was obtained after two intermediary signal - processing steps: filtering and windowing. The same signal processing process was applied to the reference and to the reflected signals.
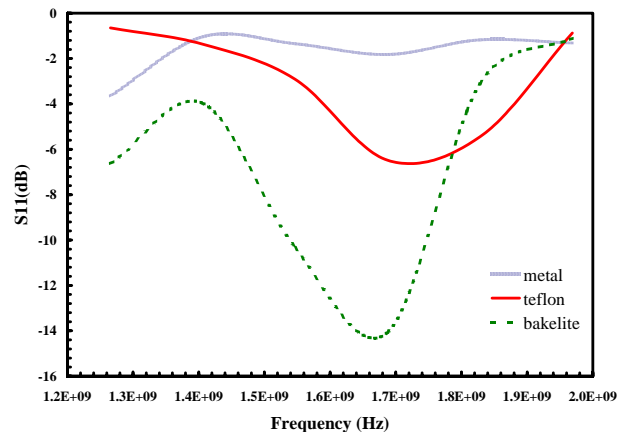
Figure 3. S_{11} parameter extracted from the TLM generated signals for different materials.

Figure 4 shows the numerical results for simulation of scanning over two small pieces of bakelite and teflon respectively. The length of the dielectric pieces was 1.6 mm and the step size in scanning was 0.033 mm. The dielectric profiles were obtained by selecting the corresponding computed S_{11} parameter for 1.72 GHz. This procedure is

identical to that used in experimental microwave microscopy [15].
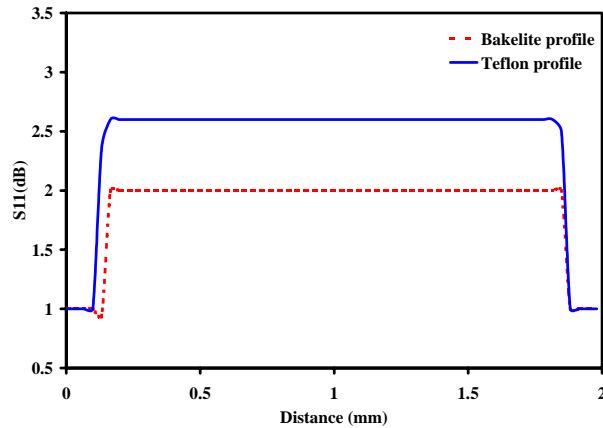
Figure 4. Results of numerical scanning for two pieces of dielectric.

The results obtained prove that the TLM algorithm can be used to model detection of local variation in permitivity. Furthermore, the TLM algorithm presented in this paper can be implemented as the forward solution subroutine for the reconstruction of the permitivity profile. A reconstruction process of inhomogenities in permitivity based on a Newton's iterative scheme for microwave imaging was proposed before [16]. This reconstruction code will involve the following steps:

1. Computing the electric fields using the TLM algorithm described here for each of the different excitations, initially assuming a homogeneous sample.
2. Obtaining the difference between the measured and computed fields (determined in step 1) at a finite number of locations for a finite number of incident fields.
3. Constructing the Jacobian matrix required in the Newton's method [17].
4. Computing a perturbation of complex valued wave number squared, Δk^2.
5. Modifying the values of k^2 based on the computed Δk^2 and repeating steps 1-4 until a convergence criteria is satisfied.

V. ACKNOWLEDGEMENT

VI. CONCLUSIONS

A numerical model for scanning microwave microscopy was implemented. The model is based on the TLM algorithm. The results shown in this paper demonstrate that the models can be applied to the dimensional characterization of structures with different electric permittivities. The scanning process was also implemented in the numerical model. The results obtained show that the numerical model can be run in parallel with the experimental scanning. This allows a better characterization of reflectors detected by microwave microscopy. Using TLM algorithm in reconstruction of permittivity profiles based on microwave measurements is proposed in this article.

REFERENCES

[1] Ida N. " Microwave NDT" Kluwer Press, 1992
[2] Johns, P. B. Beurle, R. L." Numerical solution of Two-Dimensional Scattering Problems Using a Transmission-Line Matrix" *Proc. IEEE,* vol 118, pp. 1203-1209, 1971.
[3] Sadiku, M.N.O.; Obiozor, C.N. "A comparison of finite difference time-domain (FDTD) and transmission-line modeling (TLM) methods", Southeastcon 2000. Proceedings of the IEEE pp: 19 –22, 2000.
[4] Porti, J.A Morente "TLM method and acoustics" *International Journal of numerical modeling*, Vol 14, pp.171-183 2001.
[5] Johns P. B. "A symmetrical condensed node for the TLM method ", *IEEE transaction on Microwave theory and techniques* vol. MTT_35 No.4 pp370-377, 1987.
[6] Krumpholz, M., Russer, P. "A field theoretical derivation of the transmission line method" *IEEE transaction on Microwave theory and techniques* Vol.42 No. 9. pp. 1660-1668, 1994.
[7] Krumpholz, M., Russer, P. " Discrete time-domain Green's function for three dimensional TLM modeling of the radiating boundary conditions "Applied Computation Electromagnetic Society, Monterey, CA, pp. 458-466, 1993.
[8] So, P.M., Woefer, W.J.R."A new look at the 3D condensed node TLM scattering″ *Microwave Symposium Digest, IEEE MTT-S International* vol.3 pp.1443-1446, 1993.
[9] Russer, P., Krumpholz, M. " The Hilbert space formulation of the TLM method" *International journal of numerical modelling: Electronic Networks, Devices and Fields,* Vol.6, No.1, pp.29-45, 1993.
[10] Ciocan, R. "Numerical models for elastic and electromagnetic waves propagation with applications to nondestructive characterization of materials", Ph.D. thesis, The University of Akron, May 2003.
[11] Hoefer W.J.R., So P.M., *The electromagnetic wave simulator*, John Wiley & Sons, 1993.
[12] Tong C. E., Fujino, Y. " An efficient algorithm for transmission line matrix analysis for electromagnetic problems using the symmetrical condensed node", *IEEE Trans. Microwave Theory Tech,* Vol. MTT-39, No.8 pp. 1421-1424, 1991.
[13] Trenkic, V., Christopoulos, C., Benson T.M. "Theory of the symmetrical Super-condensed node for the TLM method" *IEEE Trans. Microwave Theory Tech,* Vol. MTT-43, No. 6, pp. 1342-1348, 1995.
[14] Herring J. L. "Developments in the transmission-Line modelling method for electromagnetic compatibility studies" Ph.D thesis University of Nottingham, May 1993.
[15] Ciocan, R. Tabib-Azar, M. "Transient thermography of semiconductors using Microwave Microscope", *Microscale Thermophysical Engineering* Vol. 3 (4), pp .321-327, 1999.
[16] Meaney P.M., Paulsen K. D., Ryan, T.P. "Two dimensional hybrid element image reconstruction for TM illumination" IEEE transaction on antennas and propagation Vol. 43, No. 3, March, pp.239-247, 1995.
[17] Jiang, H., Keith D., Osterberg, U. " Optical image reconstruction using frequency domain data: simulation and experiments", J. Opt. Soc. Am. A. Vol. 13 No. 2 pp. 253-266, 1996.

Razvan Ciocan is currently a postdoctoral fellow in the Physics and Astronomy Department at Clemson University, Clemson, SC, USA. He got his PhD in Electrical Engineering at the University of Akron, OH, USA. He received the MS in Electrical Engineering from Case Western Reserve University, Cleveland, OH, USA and the BS in Applied Physics from University of Bucharest, Romania. His research focuses on microwave and ultrasonic imaging.

Nathan Ida is currently Professor of electrical engineering at The University of Akron, Akron, Ohio, USA, where he has been since 1985. His current research interests are in the areas of numerical modeling of electromagnetic fields, electromagnetic wave propagation, nondestructive testing of materials at low and microwave frequencies and in computer algorithms. Dr. Ida received his B.Sc. in 1977 and M.S.E.E. in 1979 from the Ben-Gurion University in Israel and his Ph.D. from Colorado State University in 1983.

Eugenia Ciocan received her Ph.D. degree at the "Al. I Cuza" University, Iasi, Romania in 1998. She worked in numerical modeling of heat and mass transport phenomena at the Institute for Nuclear Research, Pitesti and in optical characterization of materials at Case Western Reserve University, Cleveland, Ohio, USA. Her current research interests include the application of the numerical methods in electromagnetics and elastic wave propagation

Huabei Jiang is a Professor of physics at Clemson University, Clemson, SC, USA. His research interests include biomedical applications of model-based optical, microwave and ultrasonic imaging. Dr. Jiang received his first PhD in 1988 from the University of Electronic Science and Technology of China, Chengdu, China, and his second PhD in 1995 from Dartmouth College, Hanover, NH, USA

.